Jean Noël Nyemb*, Shafi Ullah Khan, Isaac Silvère Gade, Gaétan Bayiha Ba Njock, Paul Sakava, Lafya Bodeboret Djimtoingar, Samuelson Martin Luther King Boum Bindebe, Alex De Theodore Atchadé, Emmanuel Talla and Marcello Iriti*

In silico inhibition mechanism of *α*-amylase and *α*-glucosidase by fragransinic acid and bellericagenin B, two compounds from *Combretum fragrans* F. Hoffm (Combretaceae)

https://doi.org/10.1515/znc-2025-0193
Received August 30, 2025; accepted February 4, 2026;
published online February 25, 2026

Abstract: Diabetes mellitus remains a global health challenge, necessitating novel therapeutic strategies to manage postprandial hyperglycemia. Inhibition of carbohydrate-hydrolyzing enzymes represents a key approach. This study investigates the inhibitory potential of phytochemicals from *Combretum fragrans*, a Cameroonian medicinal plant traditionally used for diabetes, against these enzymes. Five triterpenoids fragransinic acid (**1**), betulin (**2**), betulinic acid (**3**), bellericagenin B (**4**), and a mixture of *β*-sitosterol (**5**) and stigmasterol (**6**) were evaluated via molecular docking using HYBRID and FRED protocols. The crystal structures of *α*-amylase (PDB ID: 1B2Y) and *α*-glucosidase (PDB ID: 2QMJ) were prepared, and acarbose served as a reference inhibitor. Docking validation confirmed the reliability of the protocols (RMSD < 2 Å). Compounds **1** and **4** exhibited notable binding affinities, with HYBRID scores of −5.6 and −3.7 kcal/mol for *α*-glucosidase, and −8.1 and −7.3 kcal/mol for *α*-amylase, respectively. Key interactions included hydrogen bonds with catalytic residues (ASP443, THR205) and extensive Pi–alkyl interactions with aromatic residues (TYR299, TRP539, PHE575). All the compounds demonstrated selective binding modes, suggesting competitive inhibition. This study highlights the potential of *C. fragrans* triterpenoids as *α*-amylase and *α*-glucosidase inhibitors, providing a structural basis for further phytochemical optimization in anti-diabetic drug discovery.

Keywords: diabetes; hyperglycemia; triterpenoids; enzymatic inhibition

1 Introduction

Nowadays, diabetes mellitus (DM) remains among the most debatable public health issues in the whole world. It is a metabolic disorder caused by lower secretion of insulin by pancreatic *β*-cells, or poor responses of organs to insulin [1, 2] leading to hyperglycemia, glycosuria, and sometimes ketonemia [3]. At long term, complications of DM include retinopathy, neuropathy, and microangiopathy [4]. Control of hyperglycemic condition through the inhibition of *α*-amylase and *α*-glucosidase, two carbohydrate hydrolyzing enzymes, remains one of the best strategies for the treatment of DM. Indeed, the inhibition of those enzymes leads to the decrease of the starch hydrolysis rate and, therefore, prevents a sudden surge in glucose, thereby lowering post-prandial hyperglycemia [4, 5]. Medicinal plants are an alternative to oral hypoglycemic medication such as acarbose, metformin, sulfonylureas, thiazolidinediones, biguanides, meglitinides, and dipeptidyl peptidase-IV inhibitors, due to their low toxicity, specificity, target affinity, and abundance [6, 7].

Jean Noël Nyemb and Shafi Ullah Khan equal first author contribution.

***Corresponding authors: Jean Noël Nyemb**, Department of Refining and Petrochemistry, National Advanced School of Mines and Petroleum Industries, The University of Maroua, Kaele 08, Cameroon, E-mail: nyembjeannoel@gmail.com; and **Marcello Iriti**, Department of Biomedical, Surgical and Dental Sciences, University of Milan, 20129 Milan, Italy; and National Interuniversity Consortium of Materials Science and Technology (INSTM), 50121 Firenze, Italy, E-mail: marcello.iriti@unimi.it. https://orcid.org/0000-0002-5063-1236 (M. Iriti)
Shafi Ullah Khan, UNICAEN, Inserm U1086 ANTICIPE (Interdisciplinary Research Unit for Cancer Prevention and Treatment), Normandie University, Caen, France; and Cancer Centre François Baclesse, UNICANCER, Caen, France
Isaac Silvère Gade and Gaétan Bayiha Ba Njock, Department of Chemistry, Faculty of Science, The University of Maroua, Maroua, Cameroon
Paul Sakava, Department of Chemistry, Higher Teacher Training College, The University of Bamenda, P.O. Box 39 Bambili, Cameroon
Lafya Bodeboret Djimtoingar, **Samuelson Martin Luther King Boum Bindebe and Emmanuel Talla,** Department of Chemistry, Faculty of Science, The University of Ngaoundere, P.O. Box 454, Ngaoundere, Cameroon
Alex De Theodore Atchadé, Department of Organic Chemistry, Faculty of Science, The University of Yaoundé I, Yaoundé, Cameroon

Combretum fragrans F. Hoffm is among one of the antidiabetic herbs used by traditional healers in the Far North Region of Cameroon. It belongs to *Combretum* genus, a genus of about 250 plant species and considered as the richest genus of the Combretaceae family. A number of *Combretum* species are used for the treatment of several types of diseases, among which mental problems, microbial infections, snake and scorpion bites, fever, heart problems, and worm remedies [8]. Apart from diabetes mellitus, *C. fragrans* is also used to treat hypertension, inflammation, syphilis, leprosy, diarrhea, incurable wound, malaria, septic wounds, coughs, fungal infection of the scalp, gonorrhea, and snake bite [9–12]. To the best of our knowledge, till date, there are no reports on scientific validation of the traditional claim of this plant against diabetes mellitus. Recently, our previous study on the crude methanolic extract of the stem bark of this plant led to the isolation of fragransinic acid (**1**), betulin (**2**), betulinic acid (**3**), bellericagenin B (**4**), and a mixture of *β*-sitosterol (**5**) and stigmasterol (**6**). The present study aims to establish a structure–activity of those previous isolated compounds against *α*-glucosidase and *α*-amylase activity compared to acarbose, a known inhibitor of these enzymes. Molecular docking was then performed to predict the binding model of these compounds to the 3D structure of both enzymes, *α*-glucosidase and *α*-amylase.

2 Materials and methods

2.1 Plant material collection, extraction, and compound isolation

The stem barks of *C. fragrans* F. Hoffm collected in May 2017 in the North Region of Cameroon, precisely at Padarmé in the Bibémi subdivision, were identified at the National Herbarium of Cameroon (39753/HNC).

Extraction and compounds isolation were done according to our previous report study [9]. Indeed 1 kg of powdered stem bark of *C. fragrans* was macerated in MeOH (3 L) for 48 H. The macerate was further filtrated and evaporated under reduced pressure on rotary evaporator to afford a brown dark crude extract. The operation has been repeated three times, leading 40 g of crude MeOH extract. About 30 g of this extract was separated by successive column chromatography on silica gel using hexane–EtOAc (1:0–0:1) and EtOAc–MeOH (1:0–0:1) as eluent. This led to the isolation of fragransinic acid (**1**), betulin (**2**), betulinic acid (**3**), bellericagenin B (**4**), and a mixture of *β*-sitosterol (**5**) and stigmasterol (**6**) (Figure 1) [9].

2.2 Selection and preparation of target protein structures

The crystal structures of *α*-amylase (PDB ID: 1B2Y) and *α*-glucosidase (PDB ID: 2QMJ) were retrieved from the RCSB Protein Data Bank. The structures were then prepared for molecular modeling studies using Discovery Studio Client software. Prior to molecular docking, water molecules and nonprotein residues were removed from the protein structures to improve computational efficiency and focus on the protein core. The electrostatic potential of the protein structures was improved by assigning appropriate partial charges to each atom. This was done using a force field–based approach that considers the atomic types, bond lengths, and angles. Hydrogen atoms were added to the protein structures to complete their chemical structures. This was necessary for accurate protein–ligand interactions and to ensure that the structures were consistent with the atomic coordinates provided in the crystal structure files. Acarbose, a cocrystal ligand of both selected protein *α*-amylase and *α*-glucosidase, was utilized. Acarbose is a potent inhibitor of *α*-amylases and is, therefore, considered a good candidate for validating and defining the active site residues. The active sites were delineated based on the interaction regions with acarbose, focusing on residues within a 10 Å radius of the ligand. This was done using the Make Receptor tool in OpenEye Scientific Software, which automatically identifies and selects residues based on their proximity to the ligand.

2.3 Selection and preparation of compounds from *Combretum fragrans* for molecular docking

A total of five compounds were selected from *C. fragrans* for molecular docking as potential inhibitors against alpha amylase and alpha glucosidase. These compounds underwent prerequisite ligand preparation prior to molecular docking. FRED and HYBRD require a set of input conformers for each compound. Prerequisite multiconformer generation of the compound library was performed using the OMEGA tool in OpenEye Scientific Software. OMEGA generates energy-minimized molecular structures, including their tautomers, ionization states, ring conformations, and stereoisomers, to produce a broad range of chemical and structural diversity from a single input structure. Therefore, we utilized all of OMEGA's functionalities to prepare our dataset for subsequent molecular docking simulations.

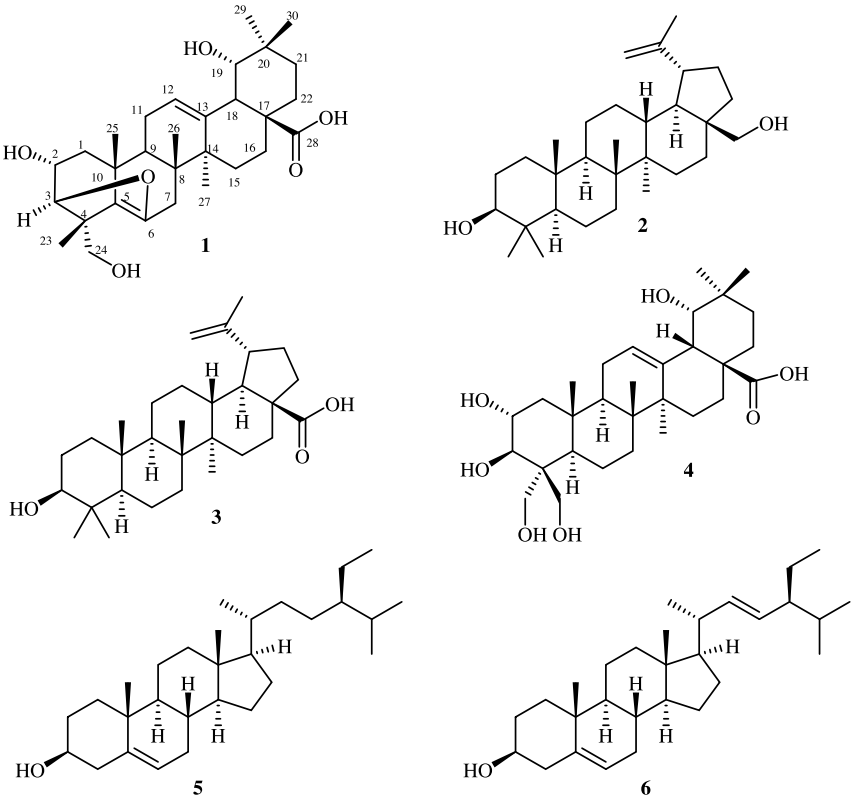

Figure 1: Structures of triterpenoids identified in *C. fragrans*.

2.4 Validation of molecular docking protocol

Prior to docking of all compounds within the active site of *α*-amylase and *α*-glucosidase, the molecular docking protocol was optimized using the cocrystallized ligand acarbose. To validate the docking protein, the bound acarbose was extracted and redocked within the *α*-amylase and *α*-glucosidase targets. Two different molecular docking approaches, FRED and HYBRID, implemented in OpenEye Scientific Software, were used to optimize subsequent virtual screening conditions.

2.5 Molecular docking protocol

After generating prerequisite compound structures from *C. fragrans* and preparing the target enzyme structures (*α*-amylase and *α*-glucosidase), virtual screening was performed to determine the putative binding interactions of the compounds with each target enzyme. Based on the validation of the molecule docking protocol in the previous step, HYBRID v 3.2.0.2 from OpenEye Scientific Software was used to perform the virtual screening of the compounds with *α*-amylase and *α*-glucosidase. HYBRID's default parameters were used for the docking calculation of all compounds within the active sites of *α*-amylase and *α*-glucosidase. HYBRID generated 10 poses for each compound, and the pose with the lowest HYBRID chemguass4 score was selected for further analysis. Binding interactions of the best-docked poses were visualized using Discovery Studio v16.0.

2.6 *In silico* pharmacokinetic and toxicity prediction

Pharmacokinetic and toxicity properties of the compounds (**1**–**4**, and **6**) were predicted using DataWarrior software. The in silico analysis focused on key molecular descriptors and prediction models inherent to the DataWarrior platform. The properties calculated include molecular weight (g/mol), theoretical partition coefficient (cLogP), theoretical aqueous solubility (cLogS), counts of hydrogen bond acceptors (H-Acceptors) and donors (H-Donors), polar surface area (PSA in $Å^2$), and drug-likeness score. Additionally, potential toxicity profiles, including mutagenicity, tumorigenicity, and reproductive effectiveness, were assessed through predictive models within DataWarrior. It is important to note that these predictions serve as preliminary indicators.

3 Results

3.1 Compounds isolation

Compounds isolation from the stem barks methanol crude extract of *C. fragrans* F. Hoffm led to the isolation of four pure compounds belonging to the family of triterpenoids and a mixture of steroids. Structural elucidation of those compounds was done using extensive NMR 1 & 2D data and MS data analysis coupled with the comparison of these spectroscopic data with those reported in the literature. Thus, among triterpenoids, fragransinic acid (**1**) [9], betulin (**2**) [13], betulinic acid (**3**) [14], and bellericagenin B (**4**) [15] have been identified. At the same time, the mixture has been identified as *β*-sitosterol (**5**) and stigmasterol (**6**) [16]. The structures of these compounds are presented in Figure 1.

3.2 Docking study

The molecular docking protocol was validated by redocking the cocrystallized ligand acarbose into the active sites of *α*-amylase and *α*-glucosidase. The validation results showed that both FRED and HYBRID docking approaches are capable of accurately docking acarbose into the active sites of these enzymes as shown in Figure 2. The docking protocols were then used to screen five compounds from *C. fragrans* as potential inhibitors of *α*-amylase and *α*-glucosidase. The docking scores for each compound were ranked, and the top-scoring compounds were selected for further investigation as shown in Table 1. The top-scoring compound from the FRED and HYBRID docking simulation revealed very crucial interaction within active site of *α*-amylase and *α*-glucosidase. These results demonstrate that molecular docking can be a valuable tool for identifying potential inhibitors of *α*-amylase and *α*-glucosidase. The docking results also revealed some insights into the binding modes of the compounds with the target enzymes. These findings suggest that the five compounds from *C. fragrans* have the potential to be developed into novel inhibitors of *α*-amylase and *α*-glucosidase.

The results of this study (Figure 3) demonstrate that the interaction of fragransinic acid (**1**) with the protein involves a variety of noncovalent interactions, including carbon hydrogen bonds, conventional hydrogen bonds, Pi–alkyl interactions, and alkyl interactions (Table 2). These interactions contribute to the stability and specificity of the protein–compound complex. The carbon hydrogen bonds are likely important for stabilizing the interaction between the protein and the compound. These bonds are formed between the carbonyl oxygen atom of the Asp443 residue and the hydrogen atom of the Histidine58 residue of the compound. Conventional hydrogen bonds are also likely important for stabilizing the interaction between the protein and the compound. These bonds are formed between the oxygen atoms of the Thr205 and Asp443 residues and the hydrogen atoms of the Aspartate443 and Histidine58 residues of the compound, respectively. The Pi–alkyl interactions are likely important for increasing the specificity of the interaction between the protein and the compound. These interactions are formed between the aromatic rings of the tyrosine residues (A:TYR299, A:TRP539, A:TRP441,

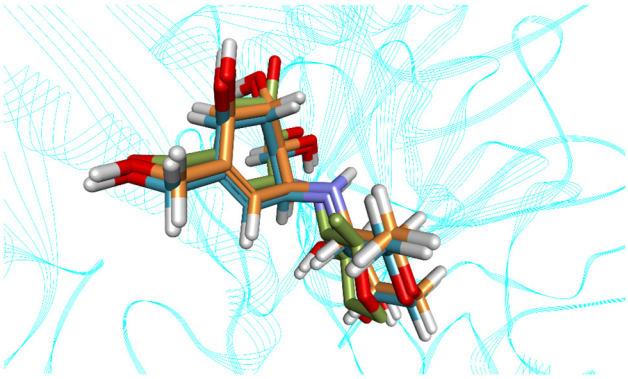

Figure 2: Illustrates a comparison of the cocrystallized ligand binding mode with the poses obtained using two different docking protocols, HYBRID and FRED. The cocrystallized ligand, shown in cyan, occupies a well-defined binding pocket within the active site of *α*-glucosidase. The HYBRID docking pose, depicted in olive, closely resembles the cocrystallized structure, while the FRED docking pose, depicted in golden, displays some deviations.

Table 1: HYBRID and FRED docking scores of compounds **1**–**4**, **6** and the reference with the human pancreatic *α*-amylase (PDB ID: 1B2Y) and *α*-glucosidase (PDB ID: 2QMJ).

	α-Glucosidase		*α*-Amylase	
Compound code	**HYBRID (kcal/mol)**	**FRED (kcal/mol)**	**HYBRID (kcal/mol)**	**FRED (kcal/mol)**
Fragransinic acid (**1**)	−5.6	−6.1	−8.1	−9.9
Betulin (**2**)	−4.1	−4.9	−7.7	−9.0
Betulinic acid (**3**)	−5.2	−5.8	−8.5	−9.1
Bellericagenin B (**4**)	−3.7	−4.7	−7.3	−8.3
Stigmasterol (**6**)	−4.4	−6.6	−9.8	−11.4
Acarbose	−11.21	−11.04		
Resveratrol	−8.8	−9.0	−8.4	−10.5
Quercetin	−7.7	−8.6	−11.0	−11.5

A:TRP406, A:PHE575, A:HIS600) and the carbon atoms of the alkyl groups of the compound (compound **1**:C25 and compound **1**:C28). The alkyl interaction is likely important for further stabilizing the interaction between the protein and the compound. This interaction is formed between the carbonyl carbon atom of the Ala576 residue and the methyl carbon atom of the compound.

Table 3 reveals a diverse range of interactions between *α*-amylase and bellericagenin B (**4**), encompassing Pi–alkyl interactions, alkyl interactions, and conventional hydrogen bonds. Pi–alkyl interactions emerge as the predominant type, potentially playing a pivotal role in compound 4's binding to alpha amylase. While conventional hydrogen bonds are less prevalent, they may still contribute to stabilizing the complex.

Analysis of binding interaction between bellericagenin B (**4**) and amino acid residue of *α*-amylase indicates that three conventional hydrogen bonds between bellericagenin B (**4**) and *α*-amylase. The interacting residues, ASP327 and THR205, engage with compound **4**'s atoms H38 and H39 moieties. Distances between interacting residues and moieties fall within the expected range for hydrogen bonds. Further analysis reveals that there are 13 Pi–alkyl interactions between compound **4** and *α*-amylase. HIS600, PHE450, PHE575, TRP406, and TYR299 serve as interacting residues, while C32, C34, C29, and C32 constitute compound **4**'s interacting moieties. The short distances between interacting residues and moieties suggest strong interactions. The average distance of approximately 4.9 Å closely aligns with the average distance for Pi–alkyl interactions. These Pi–alkyl interactions are likely to be crucial for compound **4**'s binding to *α*-amylase.

3.3 Results predicted pharmacokinetic and toxicity properties

The predicted pharmacokinetic and toxicity properties for the specified compound IDs are presented in Table 4.

The *in silico* analysis reveals several key insights into the properties of these compounds. All five compounds (**1**–**4**, and **6**) were predicted to have no mutagenic, tumorigenic, or reproductive effective properties, indicating a favorable preliminary toxicity profile *in silico*.

Molecular Weight and Lipophilicity: The molecular weights of the compounds range from 414.715 g/mol (**2**, **6**) to 520.704 g/mol (**3**). Most compounds, notably compounds **1**, **2**, **4**, and **6**, exhibit high cLogP values (ranging from 6.3706 to 7.8552). This suggests a high degree of lipophilicity, which could impact their absorption and distribution within biological systems. Conversely, **3** displays a comparatively lower cLogP (2.5067).

Aqueous Solubility and Drug-likeness: Consistent with their high cLogP values, **1**, **2**, **4**, and **6** show very low predicted aqueous solubility (cLogS values ranging from −6.278 to −6.669). Compound **3** demonstrates a slightly higher, though still low, cLogS value of −4.316. The drug-likeness scores vary among the compounds, with compounds **1** and **4** having significantly negative scores (−21.49 and −23.933, respectively), while compounds **2**, **3**, and **6** have

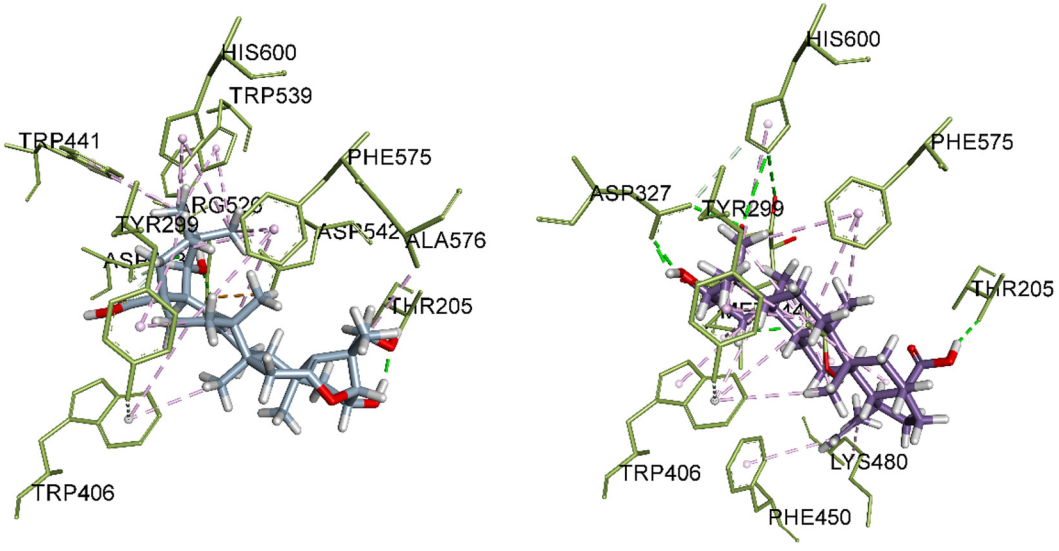

Figure 3: Binding orientation and interactions of fragransinic acid (**1**) (left) and bellericagenin B (**4**) (right) within the active site of *α*-glucosidase.

Table 2: Interaction ranges between *α*-glucosidase and fragransinic acid (**1**).

Types	Distance	Interacting amino acid residue	Interacting moiety of compound
Carbon hydrogen bond	2.37	A:ASP443:OD2	Fragransinic acid (**1**): H58
Conventional hydrogen bond	2.02	A:THR205:OG1	Fragransinic acid (**1**): H41
Conventional hydrogen bond	2.98	A:ASP443:OD1	Fragransinic acid (**1**): H39
Conventional hydrogen bond	2.64	A:ARG526:NH1	Fragransinic acid (**1**): O24
Pi–alkyl	3.37	A:TYR299	Fragransinic acid (**1**)
Pi–alkyl	4.80	A:TYR299	Fragransinic acid (**1**)
Pi–alkyl	4.45	A:TRP539	Fragransinic acid (**1**):C25
Pi–alkyl	4.66	A:TRP539	Fragransinic acid (**1**): C25
Pi–alkyl	5.27	A:TRP539	Fragransinic acid (**1**): C28
Pi–alkyl	4.35	A:TRP441	Fragransinic acid (**1**): C25
Pi–alkyl	5.12	A:TRP441	Fragransinic acid (**1**): C25
Pi–alkyl	4.20	A:TRP406	Fragransinic acid (**1**): C29
Pi–alkyl	5.12	A:TRP406	Fragransinic acid (**1**)
Pi–alkyl	3.50	A:PHE575	Fragransinic acid (**1**): C28
Pi–alkyl	4.26	A:PHE575	Fragransinic acid (**1**)
Pi–alkyl	5.01	A:PHE575	Fragransinic acid (**1**)
Pi–alkyl	5.49	A:PHE575	Fragransinic acid (**1**)
Pi–alkyl	4.28	A:HIS600	Fragransinic acid (**1**): C25
Pi–alkyl	4.56	A:HIS600	Fragransinic acid (**1**)
Pi–alkyl	5.07	A:HIS600	Fragransinic acid (**1**): C28
Alkyl	3.50	A:ALA576	Fragransinic acid (**1**): C22

Table 3: Interaction ranges between *α*-amylase and bellericagenin B (**4**).

Types	Distance	Interacting amino acid residue	Interacting moiety of compound
Conventional hydrogen bond	1.66881	A: ASP327: OD1	Bellericagenin B (**4**): H38
Conventional hydrogen bond	1.66881	A: ASP327: OD1	Bellericagenin B (**4**): H38
Conventional hydrogen bond	2.56928	A: THR205: OG1	Bellericagenin B (**4**): H39
Conventional hydrogen bond	2.56928	A: THR205: OG1	Bellericagenin B (**4**): H39
Conventional hydrogen bond	2.56928	A: THR205: OG1	Bellericagenin B (**4**): H39
Pi–alkyl	5.11725	A: PHE575	Bellericagenin B (**4**): C32
Pi–alkyl	4.97831	A: TRP406	Bellericagenin B (**4**)
Pi–alkyl	4.39044	A: TRP406	Bellericagenin B (**4**)
Pi–alkyl	5.43519	A: TRP406	Bellericagenin B (**4**)
Pi–alkyl	5.05513	A: TRP406	Bellericagenin B (**4**): C24
Pi–alkyl	4.99893	A: TYR299	Bellericagenin B (**4**)
Pi–alkyl	5.1208	A: TYR299	Bellericagenin B (**4**)
Pi–alkyl	4.57287	A: TYR299	Bellericagenin B (**4**):C32
Alkyl	5.39377	A: MET444	Bellericagenin B (**4**)
Alkyl	4.1478	A: LYS480	Bellericagenin B (**4**):C35

scores closer to zero (−4.475, −3.4819, and −4.475, respectively).

Hydrogen Bonding and Polar Surface Area: Compounds **2** and **6** are characterized by a single hydrogen bond acceptor and donor, and a very low polar surface area (PSA) of 20.23 Å^2. In contrast, **3** has the highest number of hydrogen bond acceptors (7) and donors (6), alongside the largest PSA (138.45 Å^2), suggesting a more polar character.

To address the selectivity and possible off-target effects for therapeutic development, we performed a comprehensive computational assessment of the general toxicity profile and cardiotoxicity risk associated with the isolated compounds. This analysis, summarized in Table 5, assessing potential cardiotoxicity via the hERG potassium channel (Pred-hERG) revealed that the majority of tested compounds – fragransinic acid (**1**), betulin (**2**), bellericagenin B (**4**), stigmasterol (**6**), and the reference acarbose were predicted to be nonblockers. Notably, betulin (**2**) was predicted as a nonblocker with very high confidence (99.65 %), and this specific prediction fell inside the applicability domain (AD). The only compound predicted to be a blocker was betulinic acid (3), although this prediction had lower confidence (60.8 %) and was outside the AD. These predictive toxicity results complement the docking study by addressing critical safety considerations, highlighting that most *C. fragrans* compounds possess a potentially acceptable initial safety window for further investigation.

4 Discussion

This section aims to interpret the molecular docking results, elucidate the underlying binding mechanisms, evaluate the predicted pharmacokinetic and toxicity profiles, and contextualize these findings within existing literature and the traditional medicinal uses of *C. fragrans*. It also

Table 4: Predicted pharmacokinetic and toxicity properties of compounds.

Compounds id	MW (g/mol)	cLogP	cLogS	H-acceptors	H-donors	PSA (Å^2)	Drug-likeness	Mutagenic	Tumorigenic	Reproductive effective
1	456.708	6.3706	−6.278	3	2	57.53	−21.49	None	None	None
2	414.715	7.8552	−6.669	1	1	20.23	−4.475	None	None	None
3	520.704	2.5067	−4.316	7	6	138.45	−3.4819	None	None	None
4	442.725	6.7202	−6.296	2	2	40.46	−23.933	None	None	None
6	412.715	7.8552	−6.669	1	1	20.23	−4.475	None	None	None

Table 5: Summary of *in silico* toxicity and Pred-hERG prediction assessment.

Compounds	Fragransinic acid (1)	Betulin (2)	Betulinic acid (3)	Bellericagenin B (4)	Stigmasterol (6)
MW (g/mol)	456.708	442.725	520.704	456.708	414.715
Pred-hERG prediction	Nonblocker	Nonblocker	Blocker	Nonblocker	Nonblocker
Prediction confidence (%)	98.78	99.65	60.8	93.61	92.55
Applicability domain (AD) status	Outside	Inside	Outside	Outside	Outside
Categorical potency	Weak blocker	Weak blocker	Moderate blocker	Weak blocker	Nonblocker
Mutagenic	None	None	None	None	None
Tumorigenic	None	None	None	None	None
Reproductive effective	None	None	None	None	None

addresses the limitations inherent to a purely *in silico* study and outlines crucial avenues for future research.

4.1 Interpretation of molecular docking results and binding affinities

The molecular docking simulations provide valuable preliminary insights into the potential inhibitory mechanisms of the isolated *C. fragrans* compounds against *α*-amylase and *α*-glucosidase. The rigorous validation of both FRED and HYBRID docking protocols, indicated by a Root Mean Square Deviation (RMSD) value of less than 2 Å for acarbose redocking, confirms the reliability of these methods for accurately predicting ligand binding poses within the enzyme active sites. This suggests that the predicted binding modes for the *C. fragrans* compounds are likely to be representative of their actual interactions.

While the isolated triterpenoids and sterol mixture (fragransinic acid (**1**), betulin (**2**), betulinic acid (**3**), bellericagenin B (**4**), and stigmasterol (**6**)) generally exhibited higher (less favorable) docking scores compared to the reference inhibitor acarbose against both *α*-glucosidase and *α*-amylase, their observed binding affinities still warrant investigation. Acarbose, a well-established potent inhibitor of these carbohydrate-hydrolyzing enzymes, consistently showed significantly lower (more favorable) docking scores (e.g., −11.21 kcal/mol with HYBRID for *α*-glucosidase and *α*-amylase). This disparity highlights acarbose's stronger predicted binding, likely attributable to its optimized structural characteristics for potent enzyme inhibition.

However, specific *C. fragrans* compounds demonstrated noteworthy predicted binding affinities. Fragransinic acid (**1**) consistently showed the most favorable docking scores among the isolated compounds against *α*-glucosidase (−5.6 kcal/mol HYBRID, −6.1 kcal/mol FRED), suggesting its particular inhibitory potential for this enzyme. For *α*-amylase, stigmasterol (**6**) exhibited the strongest predicted binding (−9.8 kcal/mol HYBRID, −11.4 kcal/mol FRED), closely followed by betulinic acid (**3**). These findings imply varying degrees of inhibitory potential and selectivity toward one enzyme over the other among the tested compounds. The observation that these compounds demonstrated selective binding modes, despite having weaker affinities than acarbose, suggests their potential for competitive inhibition.

It is crucial to acknowledge that this study is entirely computational (*in silico*) and lacks experimental validation, such as *in vitro* enzyme inhibition assays or cytotoxicity tests, which would be essential to fully confirm the biological efficacy of the compounds and validate these predicted binding affinities. Furthermore, while docking scores offer an indication of binding strength, the statistical significance of these values was not quantitatively analyzed in this study,

representing a limitation. Future research could significantly benefit from including comparisons with other known natural inhibitors (e.g., flavonoids, polyphenols) to provide a broader context for the relative efficacy of the compounds from *C. fragrans*.

4.2 Detailed analysis of binding interactions

The detailed analysis of the best-docked poses provides a molecular-level understanding of how *C. fragrans* compounds interact with the active sites of *α*-glucosidase and *α*-amylase, which is fundamental to their predicted inhibitory mechanisms.

Fragransinic acid (1) with α-glucosidase: The binding of fragransinic acid (**1**) to *α*-glucosidase involves a complex and diverse array of noncovalent interactions, including conventional hydrogen bonds, carbon hydrogen bonds, Pi–alkyl interactions, and alkyl interactions. Conventional hydrogen bonds were observed with key active site residues, notably A:THR205 (2.02 Å) and A:ASP443 (2.98 Å), which are critical for stabilizing the protein–compound complex. The interaction with A:ARG526 (2.64 Å) also contributed to hydrogen bonding. The involvement of A:ASP443 is particularly significant, as it is a conserved catalytic residue in *α*-glucosidase, implying a direct interference with enzyme function. A carbon hydrogen bond was identified at 2.37 Å between the carbonyl oxygen of A:ASP443 and a hydrogen atom of fragransinic acid (**1**) (H58), further stabilizing the interaction. Extensive Pi–alkyl interactions were a prominent feature, involving the aromatic rings of residues such as A:TYR299, A:TRP539, A:TRP441, A:TRP406, A:PHE575, and A:HIS600. These interactions, involving the alkyl groups of fragransinic acid (**1**) (C25, C28, C29), are crucial for increasing binding specificity and underscore the prominence of hydrophobic interactions within the binding pocket. An alkyl interaction at 3.50 Å between the carbonyl carbon of A:ALA576 and the methyl carbon (C22) of fragransinic acid (**1**) also contributed to stability. These multimodal interactions collectively contribute to the stability and specificity of the fragransinic acid (**1**)–*α*-glucosidase complex. The visual representation of these intricate binding orientations and interactions is provided in Figure 3.

Bellericagenin B (4) with α-amylase: Bellericagenin B (**4**) interacted with *α*-amylase through a combination of Pi–alkyl interactions, alkyl interactions, and conventional hydrogen bonds. Conventional hydrogen bonds were observed with A:ASP327 (1.66881 Å) and A:THR205 (2.56928 Å). The interaction with THR205 is noteworthy, as it is a conserved residue in *α*-amylase, further supporting the potential for competitive inhibition. Pi–alkyl interactions emerged as the predominant type and appear to be crucial for binding. These involved residues such as A:PHE575, A:TRP406, A:TYR299, A:HIS600, and A:PHE450. With an average distance of approximately 4.9 Å, these interactions emphasize the significant role of hydrophobic contacts for bellericagenin B (**4**)'s binding to *α*-amylase. Alkyl interactions were identified with A:MET444 and A:LYS480 (involving C35 of compound **4**).

The prevalence of hydrophobic interactions, particularly Pi–alkyl interactions with aromatic residues, for both fragransinic acid (**1**) and bellericagenin B (**4**), underscores the significant role of the triterpenoid lipophilicity in facilitating enzyme binding. These specific binding modes, characterized by hydrogen bonds with catalytic/conserved residues and extensive hydrophobic contacts, suggest that these compounds may act as competitive inhibitors by directly interfering with substrate binding within the enzyme active site.

4.3 Predicted pharmacokinetic (ADME) properties and toxicity profiles

The *in silico* prediction of ADME (Absorption, Distribution, Metabolism, and Excretion) properties and toxicity profiles offers a preliminary, yet critical, assessment of the potential drug-likeness and safety of the isolated compounds.

Molecular Weight (MW): The compounds range from 414.715 g/mol (betulin (**2**), stigmasterol (**6**)) to 520.704 g/mol (betulinic acid (**3**)). While some compounds are within the common range for orally active drugs (typically below 500 g/mol), betulinic acid (**3**) is slightly above, which could potentially impact oral bioavailability.

Lipophilicity (cLogP): Most compounds, including betulin (**2**) and stigmasterol (**6**) (cLogP = 7.8552), fragransinic acid (**1**) (cLogP = 6.3706), and bellericagenin B (**4**) (cLogP = 6.7202), are predicted to be highly lipophilic. While this characteristic can facilitate membrane permeability, excessive lipophilicity might lead to issues such as poor aqueous solubility and nonspecific binding, posing challenges for pharmaceutical development. Betulinic acid (**3**) presents as comparatively less lipophilic with a cLogP of 2.5067.

Aqueous Solubility (cLogS): Directly correlating with their high lipophilicity, the compounds generally exhibited low predicted aqueous solubility, with cLogS values ranging from −4.316 (betulinic acid (**3**)) to −6.669 (betulin (**2**), stigmasterol (**6**)). Low solubility is a well-known major hurdle for drug absorption and formulation.

Hydrogen Bonding Capabilities: The number of hydrogen bond acceptors (1–7) and donors (1–6) varies among the compounds. Betulinic acid (**3**) notably possesses

the highest counts (7 H-Acceptors, 6 H-Donors), contributing to its higher polar surface area.

Polar Surface Area (PSA): Values ranged from 20.23 $Å^2$ (betulin (**2**), stigmasterol (**6**)) to 138.45 $Å^2$ (betulinic acid (**3**)). PSA is an important descriptor inversely correlated with passive drug absorption across biological membranes. Values typically below 140 $Å^2$ are desirable for good oral absorption, suggesting that most compounds might possess reasonable permeability, though betulinic acid (**3**)'s higher PSA could imply poorer permeability.

Drug-likeness Score: The drug-likeness scores varied widely, from −3.4819 (betulinic acid (**3**)) to −23.933 (bellericagenin B (**4**)). These scores suggest that while betulinic acid (**3**) is somewhat "drug-like," others, particularly bellericagenin B (**4**) and fragransinic acid (**1**), might deviate significantly from established drug-like properties, which could present challenges in their development as conventional oral drugs.

Crucially, the *in silico* toxicity predictions for all tested compounds (fragransinic acid (**1**), betulin (**2**), betulinic acid (**3**), bellericagenin B (**4**), and stigmasterol (**6**)) consistently indicated "none" for mutagenicity, tumorigenicity, and reproductive effectiveness. This is a highly positive preliminary indication regarding their safety profile as potential therapeutic agents. However, it is paramount to emphasize that these are purely computational predictions and necessitate extensive experimental validation through rigorous *in vitro* and *in vivo* studies to definitively confirm their safety and pharmacokinetic behavior.

4.4 Comparison with existing literature and future directions

This study represents a significant step in the scientific validation of the traditional claim of *C. fragrans* as an antidiabetic agent, specifically through the *in silico* elucidation of its phytochemicals' inhibitory mechanisms against *α*-amylase and *α*-glucosidase. *C. fragrans* has a well-documented history of traditional uses in Cameroon for various ailments, including diabetes, hypertension, inflammation, and microbial infections. The isolation of fragransinic acid (**1**), betulin (**2**), betulinic acid (**3**), bellericagenin B (**4**), and a mixture of *β*-sitosterol (**5**) and stigmasterol (**6**) from this plant has been previously reported [9]. Apart from compounds **1** and **4**, recent research had explored the other four isolated compounds for their antidiabetic properties using not only *in vitro* models but also *in silico* and *in vivo* models [17–22]. These studies have shown that betulin (**2**), betulinic acid (**3**), *β*-sitosterol (**5**), and stigmasterol (**6**) have shown potential as an *α*-amylase and *α*-glucosidase inhibitor, suggesting their possible use in managing type 2 diabetes. *In silico* studies indicate that those compounds bind effectively to both enzymes, potentially hindering their ability to break down carbohydrates and raise blood glucose levels.

β-Sitosterol improves glycemic control through activation of IR and GLUT4 in the adipose tissue of high fat and sucrose-induced type-2 diabetic rats [17]. Rathinavelusamy et al. [18] performed *in silico* studies between *α*-amylase (HPA) and *β*-sitosterol. The study studies showed the potent inhibition of *β*-sitosterol on human pancreatic amylase (HPA) with an estimated inhibition constant (Ki) of 269.35 nmol and two hydrogen bond interactions. The molecular modeling results undoubtedly revealed *β*-sitosterol as a potential inhibitor of HPA in comparison with acarbose. Another molecular docking study using AutoDock Vina (PyRx) and SeeSAR tools identified *β*-sitosterol as an effective *α*-amylase inhibitory compound. Among the analyzed 15 phytochemicals, *β*-sitosterol demonstrated the most appreciable binding energy (−9.0 kcal/mol) and is comparatively higher than acarbose (−7.6 kcal/mol) (Ravi et al. 2024). *In vitro* enzyme inhibition and kinetics studies along with glucose uptake revealed potent antidiabetic property of stigmasterol with a competitive inhibition against *α*-amylase and a mixed inhibition against *α*-glucosidase [19]. In the same study, *in silico* studies and the analysis of docking scores of protein–ligand interaction binding studies confirmed this reactivity of stigmasterol toward these two enzymes. Moreover, ADME properties reveal suitability of stigmasterol, indicating its potential as a drug candidate for further investigation [19]. The study of Lolok and collaborators [20] that aimed to study the complex stability of stigmasterol and *β*-sitosterol toward *α*-amylase and *α*-glucosidase by employing molecular dynamics simulation showed that the affinity of *β*-sitosterol and stigmasterol to both enzymes, in terms of the total binding energy, is stronger than that of acarbose, the complexes of stigmasterol/*α*-amylase and stigmasterol/*α*-glucosidase being more stable than the one made by acarbose [20]. Betulin and betulinic acid also demonstrated *in vitro* and *in silico* inhibitory effects on *α*-amylase and *α*-glucosidase [19, 23, 24]. The ability of betulinic acid to bind with the active cavity of *α*-glucosidase and thereby prevent the access of the substrate has been demonstrated by molecular docking studies [21, 25].

This study builds upon that foundational work by investigating the molecular interactions of these specific compounds (with particular emphasis on fragransinic acid (**1**) and bellericagenin B (**4**)) with key enzymatic targets relevant to diabetes management.

The findings, particularly the notable binding affinities of fragransinic acid (**1**) and bellericagenin B (**4**) against *α*-glucosidase and *α*-amylase, respectively, coupled with their detailed interaction profiles, provide a strong structural basis for understanding their potential antidiabetic activity. While the compounds exhibited lower docking scores than the widely used antidiabetic drug acarbose, their interactions with conserved catalytic and noncatalytic residues (e.g., ASP443 in *α*-glucosidase; THR205 in *α*-amylase) strongly suggest their potential for competitive inhibition. The observed prominence of hydrophobic interactions, particularly Pi–alkyl interactions with aromatic residues, further underscores the significant role of the inherent triterpenoid lipophilicity in facilitating enzyme binding.

Despite these promising *in silico* results, the primary limitation of this study is its reliance solely on computational methods, without experimental validation. Given the limited quantity of isolated compounds, this study should, therefore, be considered as a preliminary computational investigation aimed at identifying the most promising candidates and guiding future *in vitro* validation. To advance these compounds toward preclinical evaluation for diabetes therapy, future work is essential and has been planned to perform the *in vitro* validation by conducting enzyme inhibition assays and cytotoxicity tests to experimentally confirm the predicted biological efficacy and safety profile of these compounds.

The present study provides a solid foundational understanding and a structural basis for further phytochemical optimization in antidiabetic drug discovery, particularly from natural sources like *C. fragrans*.

5 Conclusions

This *in silico* study elucidates the inhibitory mechanisms of *C. fragrans* triterpenoids against *α*-amylase and *α*-glucosidase, enzymes critical in postprandial hyperglycemia management. Molecular docking revealed that fragransinic acid (**1**) and bellericagenin B (**4**) engage with catalytic and noncatalytic residues through hydrogen bonds and Pi–alkyl interactions, mimicking acarbose's binding mode but with distinct affinity profiles. While the compounds exhibited lower docking scores than acarbose, their interactions with conserved residues (e.g., ASP443 in *α*-glucosidase; THR205 in *α*-amylase) suggest competitive inhibition potential. The prominence of hydrophobic interactions, particularly with aromatic residues, underscores the role of triterpenoid lipophilicity in enzyme binding. It is important to remind that this study represents a preliminary computational investigation intended to identify promising candidates and guide future experimental validation. These findings validate traditional claims of *C. fragrans* as an antidiabetic agent and emphasize its phytochemicals as promising scaffolds for developing natural enzyme inhibitors. Future work should prioritize *in vitro* validation, pharmacokinetic studies, and structural derivatization to enhance potency and selectivity, advancing these compounds toward preclinical evaluation for diabetes therapy.

Acknowledgments: The authors would like to thank OpenEye Scientific Software for providing us with a free license of the software.
Research ethics: Not applicable.
Informed consent: Not applicable.
Author contributions: All authors have accepted responsibility for the entire content of this manuscript and approved its submission. JNN, SUK, and MI: conceptualization, data curation, formal analysis, methodology, investigation, visualization, writing – review and editing, supervision. ISG, GBBN, PS, LBD, SMLKBB, ADTA, and ET: data curation, formal analysis, methodology, investigation, visualization, writing – original draft.
Use of Large Language Models, AI and Machine Learning Tools: None declared.
Conflict of interest: The authors state no conflict of interest.
Research funding: This project has received funding from the European Union's Horizon 2020 research and innovation programme under the Marie Skłodowska-Curie grant agreement No 101034329. Shafi Ullah Khan is the Recipient of the WINNINGNormandy Program supported by the Normandy Region.
Data availability: The raw data can be obtained on request from the corresponding author.

References

1. Galicia-Garcia U, Benito-Vicente A, Jebari S, Larrea-Sebal A, Siddiqi H, Uribe KB, et al. Pathophysiology of type 2 diabetes mellitus. Int J Mol Sci 2020;21:6275.
2. Zhu X, Liu D, Wei Q, Lin H, Zhi M, Chen Y, et al. New-onset diabetes mellitus after chronic pancreatitis diagnosis: a systematic review and meta-analysis. Pancreas 2019;48:868–75.
3. Kulkarni A, Pineros AR, Walsh MA, Casimiro I, Ibrahim S, Hernandez-Perez M, et al. 12-Lipoxygenase governs the innate immune pathogenesis of islet inflammation and autoimmune diabetes. JCI Insight 2021;6:e147812.
4. Nyemb JN, Tchuenguem RT, Venditti A, Tchinda AT, Henoumont C, Talla E, et al. Antimicrobial and *α*-glucosidase inhibitory activities of chemical constituents from *Gardenia aqualla* (Rubiaceae). Nat Prod Res 2022;36:6369–74.

5. Tolmie M, Bester MJ, Apostolides Z. Inhibition of *α*-glucosidase and *α*-amylase by herbal compounds for the treatment of type 2 diabetes: a validation of *in silico* reverse docking with *in vitro* enzyme assays. J Diabetes 2021;13:779–91.
6. Chakraborty R, Borah P, Dutta PP, Sen S. Evolving spectrum of diabetic wound: mechanistic insights and therapeutic targets. World J Diabetes 2022;13:696–716.
7. Kooti W, Farokhipour M, Asadzadeh Z, Ashtary-Larky D, Asadi-Samani M. The role of medicinal plants in the treatment of diabetes: a systematic review. Electron Physician 2016;8:1832–42.
8. Atindehou KK, Schmid C, Brun R, Koné MW, Traore D. 2004. Antitrypanosomal and antiplasmodial activity of medicinal plants from Côte d'ivoire. J Ethnopharmacol. 2004;90: 221-7.
9. Gade IS, Nyemb JN, Mahamat A, Atchade ADT, Talla E, Laurent S, et al. A novel pentacyclic triterpene acid isolated from the stem barks of *Combretum fragrans* F. Hoffm (Combretaceae). Nat Prod Res 2024;38: 1294–301.
10. Maregesi SM, Ngassapa OD, Pieters L, Vlietinck AJ. Ethnopharmacological survey of the Bunda district, Tanzania: plants used to treat infectious diseases. J Ethnopharmacol 2007;113:457–70.
11. Maima AO, Thoithi GN, Ndwigah SN, Kamau FN, Kibwage IO. Phytosterols from the stem bark of *Combretum fragrans* F. Hoffm. East Cent Afr J Pharm Sci 2008;11:52–4.
12. Mbiantcha M, Almas J, Dawe A, Faheem A, Sidra Z. Analgesic, anti-inflammatory and anti-cancer activities of Combretin A and Combretin B isolated from *Combretum fragrans* F. Hoffm (Combretaceae) leaves. Inflammopharmacology 2018;26:1429–40.
13. Prachayasittikul S, Saraban P, Cherdtrakulkiat R, Ruchirawat S, Prachayasittikul V. New bioactive triterpenoids and antimalarial activity of *Diospyros rubra*. Exp Clin Sci J 2010;9:1–10.
14. Ogunmoye A, Oladosu I, Onocha P, Choudhary I. Isolation of betulinic acid from the stem bark and root of *Uapaca guineensis*. J Res Rev Sci 2017;4:82–7.
15. Mahato SB, Nandy AK, Kundu AP. Pentacyclic triterpenoid sapogenols and their glycosides from *Terminalia bellerica*. Tetrahedron 1992;48: 2483–94.
16. Nyemb JN, Magnibou ML, Talla E, Tchinda AT, Tchuenguem RT, Henoumont C, et al. Lipids constituents from *Gardenia aqualla* Stapf & Hutch. Open Chem 2018;16:371–6.
17. Ponnulakshmi R, Shyamaladevi B, Vijayalakshmi P, Selvaraj J. *In silico* and *in vivo* analysis to identify the antidiabetic activity of beta sitosterol in adipose tissue of high fat diet and sucrose induced type-2 diabetic experimental rats. Toxicol Mech Methods 2019;29:276–90.
18. Rathinavelusamy P, Mazumder PM, Sasmal D, Jayaprakash V. Evaluation of *in silico*, *in vitro α*-amylase inhibition potential and antidiabetic activity of *Pterospermum acerifolium* bark. Pharm Biol 2014;52:199–207.
19. Hajra D, Chouni A, Paul S. Phytochemistry, antioxidant and anti-diabetic activities of *Sterculia villosa in-vitro*. Pharmacol Res Mod Chin Med 2024; 13:100530.
20. Lolok N, Sumiwi SA, Ramadhan DSF, Levita J, Sahidin I. Molecular dynamics study of stigmasterol and beta-sitosterol of *Morinda citrifolia* L. towards *α*-amylase and *α*-glucosidase. J Biomol Struct Dyn 2024;42: 1952–5.
21. Chen S, Lin B, Gu J, Yong T, Gao X, Xie Y, et al. Binding interaction of betulinic acid to α-glucosidase and its alleviation on postprandial hyperglycemia. Molecules 2022;27:2517.
22. Shahzad A, Liu W, Hussain S, Ni Y, Cui K, Sun Y, et al. Integrated *in vitro*, *in silico*, and *in vivo* approaches to lucidate the antidiabetic mechanisms of Cicer arietinum and Hordeum vulgare extract and secondary metabolites. Sci Rep 2025;15:6620.
23. Yuca H, Özbek H, Demirezer LÖ, Güvenalp Z. Assessment of the α-glucosidase and α-amylase inhibitory potential of Paliurus spina-christi Mill. and its terpenic compounds. Med Chem Res 2022;31: 1393–9.
24. Salau VF, Erukainure OL, Aljoundi A, Akintemi EO, Elamin G, Odewole OA. Exploring the inhibitory action of betulinic acid on key digestive enzymes linked to diabetes via *in vitro* and computational models: approaches to anti-diabetic mechanisms, SAR and QSAR in. Environ Res 2024;35:411–32.
25. Ding H, Wu X, Pan J, Hu X, Gong D, Zhang G. New insights into the inhibition mechanism of Betulinic acid on *α*-Glucosidase. J Agric Food Chem 2018;66:7065–75.